Trade-Offs on Fault Estimation via Proportional Multiple-integral and Multiple-resonant Observers for Discrete-time Systems

Ester Sales-Setién[1⋆] and Ignacio Peñarrocha-Alós[1]

[1]Department of Industrial Engineering and Design, Universitat Jaume I, Castellón, Spain
⋆esales@uji.es

Abstract

We develop a fault estimation strategy which is based on a novel proportional multiple-integral and multiple-resonant observer. This observer is an extension of the well-known PMI observer and it is able to estimate from low to high-frequency fault signals. The proposed estimation strategy is applied to discrete-time systems which are affected by faults and stochastic noises. We present a multiobjective design strategy of the observer that fixes the trade-offs between practical engineering parameters regarding the noise attenuation and the ability to track each kind of fault dynamics considered by the augmented observer. We study the influence of the order of the observer on the steady-state and transient performance of the estimation of different types of faults. Finally, a numerical example is given to illustrate the effectiveness of the proposed observer, design and characterization.

1 Introduction

The increasing complexity and the high costs of practical control systems impose higher demands of reliability and safety. Fault diagnosis, which has been extensively studied over the last decades [1], arises as an effective solution to meet this demand. Among fault diagnosis techniques, fault estimation (FE) appears as an advanced method that gives information not only about the moment (detection) and the location (isolation) of a fault but also about its size and shape (identification), which is of paramount importance for both real-time decision and active fault tolerant control [2].

FE can be realized by utilizing a wide variety of advanced observer techniques such as sliding mode observers [3], adaptive observers [4,5], iterative observers [6,7] and augmented observers. The essence of the latter approach is to construct an augmented system in which the faults are introduced as an additional state [8, 9]. As an extension of the Luenberger observer, proportional and integral (PI) observers, which have received much attention [10–12], assume that the faults are constant or step signals. Their applicability is thus limited to the estimation of faults whose variations are slow with respect to the dynamics of the system. By supposing the considered faults to be in the more general form of a polynomial of the time, proportional multiple-integral (PMI) observers were discussed in many works as [13–16]. However, as stated in [17], pure high-frequency fault signals cannot be covered by PMI observers. The development of strategies for estimating the parameters of sinusoidal signals turns out to be an active research area. A comparison study of the most relevant exiting methods can be found in [18]. Usually, the Fast Fourier Transform (FFT) is preferred in stationary conditions. For the estimation of sinusoidal signals with time-varying amplitudes and frequencies different kinds of adaptive techniques, as the ones presented in [19, 20], are commonly utilized.

However, in many practical applications the faults are periodic signals which can be decomposed into sinusoids of known frequencies. Take as examples the faults related to human consumption of resources such as electricity or water [21], the sensor losses of effectiveness related to the ambient temperature evolution or the faults occurring in power systems of fixed frequency [22]. If the sinusoidal frequencies are known, simpler schemes can be used and we propose to extend PMI observers in order to include this resonant dynamics.

It is noticed that FE techniques aim to simultaneously make the estimates sensitive to faults and robust against disturbances and noises [23, 24] through the accomplishment of certain trade-off between these properties [25]. In order to characterize the sensitivity of PMI observers to faults, reference works [13, 14] assume that the polynomials of the time describing the faults are of certain order and that their highest-order non-zero time-derivative

is bounded. Then, they bound the effect of these time-derivatives of highest order on the fault estimation errors. In practice, it is possible to forecast some information about the polynomial order of the faults which are prone to occur. Yet, no exact a priori knowledge of this order is available. Hence, the authors in [16, 17] propose to "choose a large order for safety". However, choosing a large polynomial order of the faults, increases the order of the corresponding augmented PMI observer and it may degrade its behaviour towards polynomial faults of lower order. It is then reasonable to ponder to what extent the increasing order of an observer improves its ability to track different type of faults; however, and to the best of the authors' knowledge, no systematic studies have been carried out in order to determine the influence of this allegedly protective election on the overall performance of the fault estimator. It seems then valuable to study the compromises resulting from such election and to provide a design strategy that allows managing the arising trade-offs. In view of this, we propose to characterize the sensitivity of PMI observers to faults by bounding the effect on the estimation error of each polynomial fault term instead of just considering the effect of the highest-order fault terms. This characterization allows designing PMI observers with a different sensitivity to each polynomial fault term according to their individual probability of appearance. Thus, for the same level of disturbance/noise attenuation, a higher ability to track the most probable forms of the fault would be achievable at the cost of a lower performance w.r.t. the less probable fault forms.

Compared with continuous-time systems, fewer and more recent results have been reported for FE in discrete-time systems [26]. In [26–28], PI estimation techniques are utilized and in [29] a PMI observer is used for disturbance estimation. It is well known that discrete-time observers are more challenging and practical than continuous-time cases because most continuous-time control systems are implemented digitally [26]. Thus, more effort has to be devoted to FE in discrete-time systems.

1.1 Contributions

Inspired by the above background, this paper uses novel proportional multiple-integral and multiple-resonant observers for FE. The paper studies the performance trade-offs that appear when using complex augmented fault observers for discrete-time systems in environments with stochastic noises and it provides a design strategy that optimally fixes these trade-offs using practical engineering parameters. In all, compared to the relevant existing literature, the main contributions of this paper are:

- *The existence conditions of proportional multiple-integral and multiple-resonant (PMIR) observers for discrete-time systems are included.* As an extension of the PI and PMI observer existence conditions available in the literature (see [16, 27]), we present the existence conditions of PMIR observers. PMIR observers represent an extension of PMI observers and they include resonant terms. Although these resonant terms are commonly utilized in power systems for building PR controllers [30, 31], PMIR observers are not utilized and their existence conditions are not available in the literature.

- *A multiobjective design of the PMIR observer based on performance trade-offs is presented.* In this paper, we present a design of the PMIR observer for systems in environments with stochastic noises. The proposed design is a multiobjective optimization problem based on matrix inequalities which fixes certain trade-off between the noise attenuation and the ability to track each fault term included in the observer. Unlike common PMI observer designs which just consider the fault tracking ability w.r.t. the highest-order time-derivative of the fault (e.g., [13, 14]), the proposed design includes the probability of appearance of each kind of fault form considered by the augmented observer and it allows specifying different tracking abilities w.r.t. each fault form.

- *Practical engineering parameters are utilized in the proposed design.* In an aim to bridging the gap between theory and practice [32], the FE perfromance is characterized by means of practical engineering parameters. The stochastic noise attenuation is represented by the variance of the estimates in fault-free scenarios and the cumulative squared errors due to fault appearances explain the fault tracking ability.

- *The performance of PMIR fault estimators when the system is subject to non-modelled faults is studied.* To reinforce the justification of the probabilistic design approach presented in this paper and provided that

no a priori exact knowledge of the dynamics of the faults affecting the system is available, we study the performance of a designed PMIR observer when the system is affected by non-modeled faults. We also study the influence of the complexity of the considered faults (i.e., the degree of the polynomial and the number of sinusoidal waves included in the augmented observer) on the performance of the estimator w.r.t. fault signals of simpler dynamics.

1.2 Structure and Notation

The outline of this work is as follows. First, we state the problem in Section 2. In Section 3, we propose a FE strategy based on a novel model-based PMIR observers and, in Section 4, we present a multiobjective optimization problem for the design of the estimator. In Section 5, we study the fault tracking ability of the estimator in both steady state and transients. A numerical example is given in Section 6. Finally, Section 7 summarizes the main conclusions and proposes future research topics.

Throughout the paper, $\mathbb{R}$ denotes the set of real numbers and $\mathbb{C}$ denotes the complex plane. Expected value, probability and absolute value are denoted by $\mathbb{E}\{\cdot\}$, $\mathbb{P}\{\cdot\}$ and $|\cdot|$. Let A be some matrix and a be some vector. $A[i,j]$ denotes the element in the i-th row and j-th column of A and $a[i]$ denotes the i-th element in a. $A \preceq 0$ means that A is negative semidefinite and similar applies to $\succeq$. The trace of matrix A is represented as $\mathrm{tr}(A)$, its rank is given by $\mathrm{rank}(A)$ and $\sigma(A)$ denotes the eigenvalues of A. Let x be a stochastic signal. We write $\|x_k\|_2^2 \triangleq x_k^T\, x_k$ for the Euclidean norm of vector x_k, $\|x\|_2^2 \triangleq \sum_{k=0}^{\infty} \|x_k\|_2^2$ for the l_2 norm of signal x and $\|x\|_{RMS}^2 \triangleq \lim_{k\to\infty} \frac{1}{K} \sum_{k=0}^{K-1} \|x_k\|_2^2$ for its RMS norm. I_n is the identity matrix of size $n \times n$ or of appropriate size when the subindex is omitted; similar applies to $0_{n\times n}$.

2 Problem Statement

Consider the linear time-invariant (LTI) discrete-time system defined by

$$x_{k+1} = A\, x_k + B\, u_k + E\, f_k + S\, w_k, \tag{1a}$$

$$y_k = C\, x_k + D\, u_k + F\, f_k + T\, w_k, \tag{1b}$$

with $x \in \mathbb{R}^{n_x}$, $y \in \mathbb{R}^{n_y}$ and $u \in \mathbb{R}^{n_u}$ being the state, output and input vector. Vector $w \in \mathbb{R}^{n_w}$ represents the noise and vector $f \in \mathbb{R}^{n_f}$ includes the faults $f[l]$ with $l = 1, \ldots, n_f$ that affect system (1). A, B, C, D, E, F, S and T are known real constant matrices of appropriate dimensions. Note that pure process noise (w^p) and pure sensor noise (w^s) may be considered by means of zeroing the appropriate columns of S and T (i.e., $w = \begin{bmatrix} w^p \\ w^s \end{bmatrix}$ with $S = \begin{bmatrix} S^p & 0 \end{bmatrix}$ and $T = \begin{bmatrix} 0 & T^s \end{bmatrix}$).The following assumptions on the system (1) are made.

Assumption 1. *The noises in w are zero-mean independent noises of known covariance, i.e., $\mathbb{E}\{w\, w^T\} = W$.*

Assumption 2. *We consider that each fault $f[l] = M_l\, f$ (with $M_l = \begin{bmatrix} 0_{1\times l-1} & 1 & 0_{1\times n_f - l} \end{bmatrix}$ and $l = 1, \ldots, n_f$) is in the fairly general form of*

$$f_k[l] = f_k^I[l] + f_k^R[l] \tag{2}$$

where $f_k^I[l] = \sum_{i=1}^{n_I} f_k^i[l]$ and $f_k^R[l] = \sum_{r=1}^{n_R} f_k^r[l]$ contain, respectively, the aperiodic and periodic components of the l-th fault which we write as

$$f_k^i[l] = \begin{cases} c_{i,l}\,(k - \kappa_{i,l})^{i-1} & \text{if } \; k \geq \kappa_{i,l} \\ 0 & \text{otherwise} \end{cases}, \tag{3a}$$

$$f_k^r[l] = \begin{cases} d_{r,l}\sin[\omega_r\,(k - \bar{\kappa}_{r,l})] & \text{if } \; k \geq \kappa_{r,l} \\ 0 & \text{otherwise} \end{cases}, \tag{3b}$$

where $c_{i,l}$ ($i = 1, \ldots, n_I$) and $d_{r,l}$ ($r = 1, \ldots, n_R$) are unknown constants, $\kappa_{i,l}$ ($i = 1, \ldots, n_I$) and $\bar{\kappa}_{r,l}$ ($r = 1, \ldots, n_R$) are the unknown times of appearance of the corresponding dynamics, and ω_r ($r = 1, \ldots, n_R$) are the discrete frequencies of the periodic components of the l-th fault.

Assumption 3. *The pair (A, C) is observable.*

Assumption 4. *The matrices A, C, E and F satisfy*

$$\operatorname{rank} \begin{bmatrix} I_{n_x} - A & -E \\ C & F \end{bmatrix} = n_x + n_f.$$

Assumption 5. *The matrices A, C, E and F satisfy*

$$\operatorname{rank} \begin{bmatrix} z\, I_{n_x} - A & -E & 0 \\ 0 & -I_{n_f} & z\, I_{n_f} \\ C & F & 0 \end{bmatrix} = n_x + 2\, n_f$$

for $z \in \{\cos(\omega_r) \pm j \sin(\omega_r)\}$ with $r = 1, \ldots, n_R$.

Remark 1. *Assumption 1 is common in systems affected by stochastic noises (e.g., Kalman filter theory).*

Remark 2. *Assumption 2 assumes certain fault dynamics and it is necessary because an augmented observer is based on an augmented model including the presumed fault dynamics [9, 28]. As in PMI observers theory [29], the term $f^I[l]$ considers aperiodic faults with bounded n_I-th time derivative. Here, we extend this approach and the term $f^R[l]$ considers high-frequency faults, which cannot be covered by PMI observers [17]*[1]*. All the fault parameters but the frequencies ω_r ($r = 1, \ldots, n_R$) are assumed to be unknown. As previously discussed, the knowledge of these frequencies is reasonable in many practical cases (e.g., electrical and power systems).*

Remark 3. *Augmented observers require the observability of the corresponding augmented model. As detailed in Section 3, Assumption 3, 4 and 5 guarantee the observability of all the eigenvalues of the model resulting from augmenting* (1) *with the fault dynamics in Assumption 2. Note that Assumption 4 is required for PMI observers including the dynamics of $f^I[l]$ and Assumption 5 extends it w.r.t. $f^R[l]$.*

The faults in the form of (2) can be modeled through

$$\xi_{k+1} = A_F\, \xi_k + B_F\, \zeta_k, \tag{4a}$$
$$f_k = C_F\, \xi_k, \tag{4b}$$

with $\xi = \begin{bmatrix} \xi^I & \xi^R \end{bmatrix}^T \in \mathbb{R}^{n_\xi}$ being the fault state vector verifying $n_\xi = n_f \cdot (n_I + 2 \cdot n_R)$ and $\xi_0 = 0$. Vector $\zeta = \begin{bmatrix} \zeta^I & \zeta^R \end{bmatrix}^T \in \mathbb{R}^{n_\zeta}$ with $n_\zeta = n_f \cdot (n_I + n_R)$ is a vector including the following impulse signals:

$$\zeta_k^I = \begin{bmatrix} c_{n_I,1}\, \delta_{k-\kappa_{n_I,1}} \\ \vdots \\ c_{n_I,n_f}\, \delta_{k-\kappa_{n_I,n_f}} \\ \vdots \\ c_{1,n_f}\, \delta_{k-\kappa_{1,n_f}} \end{bmatrix},\ \zeta_k^R = \begin{bmatrix} d_{n_R,1}\, \delta_{k-\bar{\kappa}_{n_R,1}} \\ \vdots \\ d_{n_R,n_f}\, \delta_{k-\bar{\kappa}_{n_R,n_f}} \\ \vdots \\ d_{1,n_f}\, \delta_{k-\bar{\kappa}_{1,n_f}} \end{bmatrix}.$$

[1] $f^I[l]$ can be seen as the n_I-th order Taylor series expansion at $k = 0$ for a function g whose derivatives $g^{(n)}$ exist for $n = 1, \ldots, n_I$ on $k = 0$. $f^R[l]$ with $\omega_r = r\, \omega_1$ can be seen as the n_R-th order Fourier series expansion for a periodic function g integrable on $k \in [0, 2\,\pi/\omega_1]$.

The matrices in (4) verify $A_F = \begin{bmatrix} A_F^I & 0 \\ 0 & A_F^R \end{bmatrix}$, $B_F = \begin{bmatrix} B_F^I & 0 \\ 0 & B_F^R \end{bmatrix}$, $C_F = \begin{bmatrix} C_F^I & C_F^R \end{bmatrix}$, with

$$A_F^I = \begin{bmatrix} I_{n_f} & 0 & 0 & 0 \\ I_{n_f} & I_{n_f} & 0 & 0 \\ 0 & \ddots & \ddots & 0 \\ 0 & 0 & I_{n_f} & I_{n_f} \end{bmatrix} \in \mathbb{R}^{(n_f \cdot n_I) \times (n_f \cdot n_I)},$$

$$B_F^I = I_{n_f \cdot n_I} \in \mathbb{R}^{(n_f \cdot n_I) \times (n_f \cdot n_I)},$$

$$C_F^I = \begin{bmatrix} 0 & I_{n_f} \end{bmatrix} \in \mathbb{R}^{n_f \times (n_f \cdot n_I)},$$

$$A_F^R = \left[\begin{array}{ccc|c} 2\cos(\omega_1)\, I_{n_f} & 0 & 0 & \\ 0 & \ddots & 0 & -I_{n_f \cdot n_R} \\ 0 & 0 & 2\cos(\omega_{n_R})\, I_{n_f} & \\ \hline & I_{n_f \cdot n_R} & & 0 \end{array}\right] \in \mathbb{R}^{(n_f \cdot 2 \cdot n_R) \times (n_f \cdot 2 \cdot n_R)},$$

$$B_F^R = \left[\begin{array}{ccc} \sin(\omega_1)\, I_{n_f} & 0 & 0 \\ 0 & \ddots & 0 \\ 0 & 0 & \sin(\omega_{n_R})\, I_{n_f} \\ \hline & 0 & \end{array}\right] \in \mathbb{R}^{(n_f \cdot 2 \cdot n_R) \times (n_f \cdot n_R)},$$

$$C_F^R = \begin{bmatrix} I_{n_f} & \dots & I_{n_f} & 0 \end{bmatrix} \in \mathbb{R}^{n_f \times (n_f \cdot 2 \cdot n_R)}.$$

Note that the first n_f elements in ζ refer to the generating signals related to the fault polynomial terms of highest order (i.e., $c_{n_I,l}\,(k-\kappa_{n_I,l})^{n_I-1}$). Therefore, $\zeta[l]$ refers to the polynomial term of highest order of the l-th fault and, more generally, $\zeta[(n_I-i)n_f+l]$ with $i \in [1,\dots,n_I]$ refers to the generating signal related to the term $c_{i,l}\,(k-\kappa_{i,l})^{i-1}$ of this l-th fault. In the following, we will use index m to refer to the m-th generating signal in vector ζ, index $\bar{m}(i,l) \triangleq (n_I-i)n_f+l$ to refer to the generating signal of the polynomial term of power $i-1$ in the fault channel l and index $\breve{m}(r,l) \triangleq (n_I+n_R-r)n_f+l$ to refer to the generating signal of the sinusoidal term of frequency ω_r in the fault channel l. Thus, applying the $\mathcal{Z}$ transform to (4), we get that the transfer functions $G_{f[l],\zeta[m]}(z)$ from the different generating signals $\zeta[m]$ to $f[l]$ are given in

$$f[l](z) = \sum_{i=1}^{n_I} \frac{1}{(1-z^{-1})^i}\, \zeta[\bar{m}(i,l)](z) + \sum_{r=1}^{n_R} \frac{\sin(\omega_r)\, z^{-1}}{1-2\,\cos(\omega_r)\, z^{-1}+z^{-2}}\, \zeta[\breve{m}(r,l)](z). \tag{5}$$

Remark 4. *Although the fault generator model* (4) *is built in view of the generation of fault signals in the form of* (2)*, any fault signal $f[l]$ can be generated through* (4) *by any fault input signal $\zeta[m]$ with $m = 1,\dots,n_\zeta$ whose $\mathcal{Z}$ transform is given by $\zeta[m](z) = \mathcal{Z}^{-1}\left\{G_{f[l],\zeta[m]}(z)\right\}\, \mathcal{Z}\left\{f[l]\right\}$.*

The objective of this work is to study the following problem.

Problem 1. *Given the LTI discrete-time system* (1) *with zero-mean noises and faults in the form of* (2)*, it is required to provide a design strategy of an augmented observer that allows us to optimally set the trade-offs between the noise attenuation and the individual abilities to track each polynomial and sinusoidal fault term. It is then also necessary to analyze the effect of these trade-offs on the ability to track non-modelled simpler or more complex faults.*

3 Fault Estimator

In order to build a model-based fault estimator, we extend the model (1) to include the model (4) as

$$z_{k+1} = \mathcal{A}\, z_k + \mathcal{B}\, u_k + \mathcal{E}\, \zeta_k + \mathcal{S}\, w_k, \tag{6a}$$

$$y_k = \mathcal{C}\, z_k + \mathcal{D}\, u_k + \mathcal{T}\, w_k, \tag{6b}$$

$$f_k = \mathcal{R}\, z_k, \tag{6c}$$

where $z = \begin{bmatrix} x^T & \xi^T \end{bmatrix}^T$ is the extended state vector and $\mathcal{A} = \begin{bmatrix} A & E\,C_F \\ 0 & A_F \end{bmatrix}$, $\mathcal{B} = \begin{bmatrix} B \\ 0 \end{bmatrix}$, $\mathcal{E} = \begin{bmatrix} 0 \\ B_F \end{bmatrix}$, $\mathcal{S} = \begin{bmatrix} S \\ 0 \end{bmatrix}$, $\mathcal{C} = \begin{bmatrix} C & F\,C_F \end{bmatrix}$, $\mathcal{D} = D$, $\mathcal{T} = T$ and $\mathcal{R} = \begin{bmatrix} 0 & C_F \end{bmatrix}$.

Theorem 1. *If Assumption 3, 4 and 5 are satisfied, then the extended pair $(\mathcal{A}, \mathcal{C})$ is observable.*

Proof. Define $\mathbb{O}(z) = \begin{bmatrix} z\,I_{n_x} - \mathcal{A} \\ \mathcal{C} \end{bmatrix}$. From linear systems theory, the pair $(\mathcal{A}, \mathcal{C})$ is observable if $\operatorname{rank}\{\mathbb{O}(z)\} = n_x + n_\xi$ (with $n_\xi = n_f \cdot (n_I + 2 \cdot n_R)$) for any $z \in \sigma(\mathcal{A})$. In analogy to [16, 27] and since the eigenvalues of $\mathcal{A}$ are equivalent to $\{\sigma(A), 1, \cos(\omega_1) \pm j\sin(\omega_1), \ldots, \cos(\omega_{n_R}) \pm j\sin(\omega_{n_R})\}$, this proof discusses three cases:

(i) If $z \in \sigma(\mathcal{A})$ and $z \notin \{1, \cos(\omega_1) \pm j\sin(\omega_1), \ldots, \cos(\omega_{n_R}) \pm j\sin(\omega_{n_R})\}$, we have

$$\operatorname{rank}\{\mathbb{O}(z)\} = \operatorname{rank}\begin{bmatrix} z\,I_{n_x} - A \\ C \end{bmatrix} + n_\xi$$

and, because of Assumption 3, $\operatorname{rank}\{\mathbb{O}(z)\} = n_x + n_\xi$.

(ii) If $z = 1$, we have

$$\operatorname{rank}\{\mathbb{O}(1)\} = \operatorname{rank}\begin{bmatrix} I_{n_x} - A & 0 & 0 & 0 & -E \\ 0 & I_{n_f} & 0 & 0 & 0 \\ 0 & 0 & \ddots & \ddots & 0 \\ 0 & 0 & 0 & I_{n_f} & 0 \\ C & 0 & 0 & 0 & F \end{bmatrix} + n_f 2\,n_R,$$

$$\operatorname{rank}\{\mathbb{O}(1)\} = \operatorname{rank}\begin{bmatrix} I_{n_x} - A & -E \\ C & F \end{bmatrix} + n_f\,(n_I + 2\,n_R - 1)$$

and, because o f Assumption 4, $\operatorname{rank}\{\mathbb{O}(1)\} = n_x + n_\xi$.

(iii) For any $r = 1, \ldots, n_R$, if $z = z_r$ with $z_r \triangleq \cos(\omega_r) \pm j\sin(\omega_r)$, we have

$$\operatorname{rank}\{\mathbb{O}(z_r)\} = n_f\,(n_I + 2\,n_R - 2) + \operatorname{rank}\begin{bmatrix} z_r\,I_{n_x} - A & -E & 0 \\ 0 & -\bar{z}_r\,I_{n_f} & I_{n_f} \\ 0 & -I_{n_f} & z_r\,I_{n_f} \\ C & F & 0 \end{bmatrix}. \tag{7}$$

with $\bar{z}_r$ being the complex conjugate of z_r. For $\lambda = z_r$, we have

$$-\lambda\,\bar{z}_r\,I_{n_f} + I_{n_f} = 0, \quad \lambda\,I_{n_f} - z_r\,I_{n_f} = 0;$$

because $z_r\,\bar{z}_r = 1$ and we deduce that the second and third row of the matrix in (7) are linearly dependent. Thus, it follows that

$$\operatorname{rank}\{\mathbb{O}\,(z_r)\} = n_f\,(n_I + 2\,n_R - 2) + \operatorname{rank}\begin{bmatrix} z_r\,I_{n_x} - A & -E & 0 \\ 0 & -I_{n_f} & z_r\,I_{n_f} \\ C & F & 0 \end{bmatrix}$$

and, because of Assumption 5, $\operatorname{rank}\{\mathbb{O}\,(z_r)\} = n_x + n_\xi$.

From (i), (ii) and (iii), we have that $\operatorname{rank}\{\mathbb{O}(z)\} = n_x + n_\xi$ for any $z \in \sigma(\mathcal{A})$. This completes the proof of the theorem. □

Provided the observability of the extended pair $(\mathcal{A}, \mathcal{C})$, the faults are estimated through a model-based observer in the form of:

$$\hat{z}_{k+1} = \mathcal{A}\,\hat{z}_k + \mathcal{B}\,u_k + L\,(y_k - \mathcal{C}\,\hat{z}_k - \mathcal{D}\,u_k)\,, \tag{8a}$$

$$\hat{f}_k = \mathcal{R}\,\hat{z}_k + K\,(y_k - \mathcal{C}\,\hat{z}_k - \mathcal{D}\,u_k)\,, \tag{8b}$$

where L and K are to be defined and represent the observer gain matrices that update the model-based estimations with the measurements. In analogy to the PMI observers and to the PR controllers which are used in power systems [30, 31] we say that an observer in the from of (8) is a proportional multiple-integral and multiple-resonant (PMIR) observer.

Defining the fault estimation error as $\tilde{f}_k = f_k - \hat{f}_k$ and the extended state estimation error $\tilde{z}_k = z_k - \hat{z}_k$, it follows that

$$\tilde{z}_{k+1} = \mathbf{A}\,\tilde{z}_k + \mathbf{E}\,\zeta_k + \mathbf{S}\,w_k, \tag{9a}$$

$$\tilde{f}_k = \mathbf{R}\,\tilde{z}_k + \mathbf{T}\,w_k, \tag{9b}$$

with $\mathbf{A} = \mathcal{A} - L\,\mathcal{C}$, $\mathbf{E} = \mathcal{E}$, $\mathbf{S} = \mathcal{S} - L\,\mathcal{T}$, $\mathbf{R} = \mathcal{R} - K\,\mathcal{C}$, and $\mathbf{T} = -K\,\mathcal{T}$. If we apply the $\mathcal{Z}$ transform to (9), we get

$$\tilde{f}(z) = G_{\tilde{f},\zeta}(z)\,\zeta(z) + G_{\tilde{f},w}(z) w(z), \tag{10}$$

being $G_{\tilde{f},\zeta}(z) = M(z)\mathbf{E}$, $G_{\tilde{f},w}(z) = M(z)\,\mathbf{S} + \mathbf{T}$ and $M(z) = \mathbf{R}(z\,I - \mathbf{A})^{-1}$. Note that the error sources affecting the fault estimation error are the zero-mean noises in w and the fault variations in ζ. In order to design the fault estimator (8), one must choose the observer gain matrices L and K so that certain trade-off between the attenuation from w and from ζ is satisfied.

Remark 5. *Note that the PMIR observer* (8) *enhances the estimation of simultaneous actuator and sensor faults. Redefining* $\mathcal{R}$ *as* $\mathcal{R} = \mathrm{diag}\{I, C_F\}$*, the observer* (8) *can be used as a simultaneous state and fault estimator as proposed in some works, e.g. [14, 33].*

Remark 6. *The fault estimator* (8) *could be generalized for a continuous system by augmenting the corresponding system model with the continuous form of the fault model* (4) *including continuous integrators and resonators. Then, the continuous observer should be constructed in analogy to* (8)*.*

4 Fault Estimator Design

In this section, we present an optimization-based design strategy of the observer (8). First, the robustness and the fault sensitivity of the observer, represented by norm-bounds regarding the attenuation from the noise w and from each $\zeta[m]$, are formulated using matrix inequalities. Second, these matrix inequalities are numerically transformed so that they can be implemented in a convex optimization design problem. Third, the obtained results are utilized in optimization-based problems for the design of the observer (8).

4.1 Formulation via Matrix Inequalities

The robustness and the fault sensitivity of the observer (8) are translated into norm-bounds using the formulation based on matrix inequalities in the following theorem.

Theorem 2. *Consider the fault estimator* (8) *applied to the system* (6) *and let* Γ *and* Υ *be certain diagonal matrices. If there exist any matrices* L *and* K *and any symmetric matrices* Q *and* P *fulfilling the matrix inequalities*

$$Q \succ 0, \tag{11a}$$

$$\mathbf{A}^T\,Q\,\mathbf{A} - Q + \mathbf{R}^T\,\mathbf{R} \prec 0 \tag{11b}$$

$$\mathbf{S}^T\,Q\,\mathbf{S} + \mathbf{T}^T\,\mathbf{T} - \Gamma \prec 0 \tag{11c}$$

$$P \succ 0, \tag{12a}$$
$$\mathbf{A}^T P \mathbf{A} - P + \mathbf{R}^T \mathbf{R} \prec 0 \tag{12b}$$
$$\mathbf{E}^T P \mathbf{E} - \Upsilon \prec 0 \tag{12c}$$

the following statements hold :

(i) In the absence of faults and noises (i.e., $\zeta = 0$, $w = 0$), the error (9) *converges to zero.*

(ii) In the absence of faults (i.e., $\zeta = 0$), error (9b) *is bounded as* $\mathrm{tr}(\mathbb{E}\{\tilde{f}_k\, \tilde{f}_k^T\}) < \mathrm{tr}(\Gamma\, W)$.

(iii) In the absence of noises (i.e., $w = 0$), if ζ is an impulse, error (9b) *is bounded as* $\|\tilde{f}\|_2^2 < \sum_{m=1}^{n_\zeta} \Upsilon[m,m]\, \zeta_0^2[m]$.

Proof. Define the Lyapunov functions $V_k^Q = \tilde{z}_k^T\, Q\, \tilde{z}_k$ and $V_k^P = \tilde{z}_k^T\, P\, \tilde{z}_k$. The following items prove each statement of Theorem 2.

(i) In the absence of faults and noises, premultiplying (11b) by $\tilde{z}_k^T$ and postmultipliying by its transpose, we get

$$V_{k+1}^Q - V_k^Q < 0, \tag{13}$$

which assures that the estimation error (9) converges to zero . If we perform similar steps on the inequality (12b), we get the same result w.r.t. V^P, i.e.,

$$V_{k+1}^P - V_k^P < 0, \tag{14}$$

(ii) Premultiplying (11c) by w_k^T and postmultipliying by its transpose, summing the obtained constraint to (13) and taking expected value on the result, we get

$$\mathbb{E}\{V_{k+1}^Q\} - \mathbb{E}\{V_k^Q\} + \mathrm{tr}(\mathbb{E}\{\tilde{f}_k\, \tilde{f}_k^T\}) < \mathrm{tr}(\Gamma\, W),$$

where we have taken into account the independence between $\tilde{z}_k$ and w_k and we have applied that $\mathbb{E}\{w_k^T\, \Gamma\, w_k\} = \mathrm{tr}(\Gamma\, W)$ and $\mathbb{E}\{\tilde{f}_k^T\, \tilde{f}_k\} = \mathrm{tr}(\mathbb{E}\{\tilde{f}_k\, \tilde{f}_k^T\})$ because w_k is zero-mean and so does $\tilde{f}_k$ in the absence of faults [34]. Considering null initial conditions ($\mathbb{E}\{V_0^Q\} = 0$), adding the result from $k = 0$ to $k = K$, dividing the resulting expression by K and taking the limit when $K \to \infty$, it leads to the second statement in Theorem 2 because with (11a) we have $\mathbb{E}\{V_{K+1}^Q\} \geq 0$.

(iii) Performing similar steps over the inequalities in (12) (i.e., operations with ζ_k^T on (12c), summation of the obtained constraint to (14) and taking expected value on the result), it yields

$$\mathbb{E}\{V_{k+1}^P\} - \mathbb{E}\{V_k^P\} + \mathbb{E}\{\tilde{f}_k^T\, \tilde{f}_k\} - \mathbb{E}\{\zeta_k^T\, \Upsilon\, \zeta_k\} < 0.$$

Considering null initial conditions ($\mathbb{E}\{V_0^P\} = 0$), adding the result from $k = 0$ to $k = K$, and provided that ζ_k is an impulse (i.e., $\zeta_k = 0$ for $k \neq 0$), we get $\|\tilde{f}\|_2^2 < \zeta_0^T\, \Upsilon\, \zeta_0$ because $\mathbb{E}\{V_{K+1}^p\} \geq 0$ and $\mathbb{E}\{\tilde{f}_k^T\, \tilde{f}_k\} = \tilde{f}_k^T\, \tilde{f}_k$ since ζ_k is deterministic. Provided that matrix Υ is diagonal, we prove the third statement in Theorem 2.

□

Remark 7. *Note that the third statement in Theorem 2 bounds the norm of the fault estimation error w.r.t. each fault input $\zeta[m]$ through the diagonal term $\Upsilon[m,m]$. Hence, different values in the diagonal terms of Υ enhance a design with a different sensitivity w.r.t. each different fault input $\zeta[m]$ ($m = 1, \ldots, n_\zeta$).*

In order to give a discrete-time domain interpretation to these results, the following corollary to Theorem 2 can be used. The proof is straightforward and thus it is omitted here.

Corollary 1. *If the premises in Theorem 2 are satisfied, the following statements hold for the estimator* (8) *applied to* (6)*:*

(i) The sum of the variances of the fault estimates $\hat{f}[l]$ due to noises (i.e., $\gamma = \mathrm{tr}(\mathbb{E}\{\hat{f}_k\,\hat{f}_k^T\})$ with $f = 0$) is bounded as $\gamma < \mathrm{tr}(\Gamma\, W)$.

(ii) The cumulative squared error (CSE)[2] of the fault estimation vector $\hat{f}$ due to a unitary impulse input $\zeta[m]$ (i.e., $\upsilon_m = \|\tilde{f}\|_2^2$ with $w = 0$ and $\zeta[n] = 0$ for $n = 1, \ldots, m-1, m+1, \ldots, n_\zeta$) is bounded as $\upsilon_m < \Upsilon[m, m]$.

4.2 Numerical Treatment for Convexification

Note that the conditions in Theorem 2 are standard in norm-based designs [35,36] and their feasibility depends on the restrictiveness of the chosen values for Γ and Υ. The use of independent closed-loop Lyapunov functions Q and P guarantee a non-conservative design based on these inequalities; however, the design results in a nonlinear problem. To recover convexity without conservatively requiring all specifications to be enforced by a single Lyapunov function [37], i.e., $Q = P$, we can adopt a compromise solution by introducing a slack variable Z [35, 38]. After some Schur complement operation and performing a congruence transformation by $\begin{bmatrix} Z & 0 \\ 0 & I \end{bmatrix}$ to (11) and (12), we get the linear matrix inequalities (LMIs)

$$\begin{bmatrix} Z^\star - Q & \mathscr{A} & 0 \\ \mathscr{A}^T & Q & \mathbf{R}^T \\ 0 & \mathbf{R} & I \end{bmatrix} \succ 0, \quad \begin{bmatrix} Z^\star - Q & \mathscr{S} & 0 \\ \mathscr{S}^T & \Gamma & \mathbf{T}^T \\ 0 & \mathbf{T} & I \end{bmatrix} \succ 0, \tag{15}$$

$$\begin{bmatrix} Z^\star - P & \mathscr{A} & 0 \\ \mathscr{A}^T & P & \mathbf{R}^T \\ 0 & \mathbf{R} & I \end{bmatrix} \succ 0, \quad \begin{bmatrix} Z^\star - P & Z\,\mathbf{E} \\ \mathbf{E}^T\, Z^T & \Upsilon \end{bmatrix} \succ 0, \tag{16}$$

with $Z^\star = Z + Z^T$, $\mathscr{A} = Z\,\mathcal{A} - X\,\mathcal{C}$, $\mathscr{S} = Z\,\mathcal{S} - X\,\mathcal{T}$ and $X = Z\,L$. Here, we have taken into account that the inequality $Z\,Q^{-1}\,Z^T \succeq Z + Z^T - Q$ holds for any strictly positive definite matrix Q and any full-rank matrix Z. Note that it would also be possible to iteratively solve the inequalities (11) and (12) if we perform Schur complements and we build a sequence of problems of LMIs following different approaches such as the ones presented in [39].

4.3 Design Optimization Problem

The results in Theorem 2 could be utilized to design a PMIR observer with a fixed performance w.r.t. noises and faults. In order to solve Problem 1, we use them in an optimization-based design strategy that ensures certain optimal trade-off between the robustness and the individual fault sensitivity of the observer. Let us first introduce the following assumption on the fault input vector ζ.

Assumption 6. *There is a non-zero probability that some fault inputs $\zeta[m]$ are zero, i.e., $\mathbb{P}\left\{\bigcup_{m=1}^{n_\zeta} \zeta[m] = 0\right\} \neq 0$.*

Provided Assumption 6, we can define the probability of appearance of certain fault input $\zeta[m]$ as $\alpha_m = 1 - \mathbb{P}\{\zeta[m] = 0\}$.

Remark 8. *Assumption 6 enhances PMIR observer designs in which the fault sensitivity towards the most probable fault forms is preponderant over the fault sensitivity towards less probable fault forms. Hence, the probability of appearance of the faults can be seen as design weights which are given to the different polynomial and sinusoidal fault terms in* (2)*.*

[2] The CSE experienced by an observer is intrinsically related to its settling time. Hence, higher CSEs imply higher settling times and vice-versa.

Remark 9. *It is extended in PMI observer theory to consider that the fault input is* $\zeta'_k = \begin{bmatrix} c_{n_I,1} & \dots & c_{n_I,n_f} \end{bmatrix}^T \delta_k \in \mathbb{R}^{n_f}$ *and to characterize the fault sensitivity by means of the attenuation from* ζ' *(e.g., theoretical works [13, 16] and practical works [40]). In this work, we extend this approach and we characterize the fault sensitivity by means of the individual attenuation not only from the higher order dynamics generated by* ζ' *but from all the dynamics generated by* ζ*. Note that Assumption 6 allows considering previous approaches which are achievable if we set* $\alpha_m = 1/n_f$ *for* $m = 1, \dots, n_f$ *and* $\alpha_m = 0$ *for* $m = n_f + 1, \dots, n_\zeta$*.*

The following two strategies show a proposal of how to use the results in Theorem 2 and Corollary 1 in a multiobjective optimization problem for designing fault estimators guaranteeing certain trade-off between noise attenuation and fault sensitivity. Let us remark that these design strategies are based on the discrete-time parameters in Corollary 1 (variances and CSEs) which are rather intuitive for designers in practical frameworks. To enhance the individual fault sensitivity approach, we distinguish between the fault unitary impulse inputs for which an specific CSE constraint is necessary ($\zeta[m]$ such that $m \in \Omega$, $\Omega \subset [1, n_\zeta]$) and expected/weigthed CSE of the other unitary impulse inputs ($\zeta[m]$ such that $m \notin \Omega$)

Strategy 1. *Assume that we want to design an estimator* (8) *with:*

- *minimum sum of the variances of the fault estimates* $\hat{f}[l]$ *due to noises (i.e.,* γ*),*
- *certain expected CSE due to the unitary impulse inputs* $\zeta[m]$ *such that* $m \in \Omega$ *(i.e.,* $\sum_{m\in\Omega} \alpha_m \upsilon_m \leq \bar{\upsilon}$*),*
- *certain bounded CSE (i.e.,* $\upsilon_m \leq \bar{\upsilon}_m$*) due to each unitary impulse input* $\zeta[m]$ *such that* $m \in [1, n_\zeta] \backslash \Omega$*,*

To address this design, we set the following convex optimization problem

$$\begin{aligned} \text{minimize} \quad & \operatorname{tr}(\Gamma\, W) \\ \text{subject to} \quad & \sum_{m\in\Omega} \alpha_m \Upsilon[m,m] \leq \bar{\upsilon} \\ & \Upsilon[m,m] \leq \bar{\upsilon}_m, \quad m \in [1, n_\zeta] \backslash \Omega, \\ & (15), (16) \end{aligned} \tag{17}$$

along the variables Z*,* X*,* K*,* Q*,* P*,* Γ *and* Υ *and we define* $L = Z^{-1} X$*.*

Strategy 2. *Assume that we want to design a fault estimator* (8) *with:*

- *certain bounded sum of the variances of the fault estimates* $\hat{f}[l]$ *due to noises (i.e.,* $\gamma \leq \bar{\gamma}$*),*
- *minimum expected CSE due to the unitary impulse inputs* $\zeta[m]$ *such that* $m \in \Omega \subset [1, n_\zeta]$ *(i.e.,* $\sum_{m\in\Omega} \alpha_m \upsilon_m$*),*
- *certain bounded CSE (i.e.,* $\upsilon_m \leq \bar{\upsilon}_m$*) due to each unitary impulse input* $\zeta[m]$ *such that* $m \in [1, n_\zeta] \backslash \Omega$*,*

To address this design, we set the following convex optimization problem

$$\begin{aligned} \text{minimize} \quad & \sum_{m\in\Omega} \alpha_m \Upsilon[m,m] \\ \text{subject to} \quad & \Upsilon[m,m] \leq \bar{\upsilon}_m, \quad m \in [1, n_\zeta] \backslash \Omega, \\ & \operatorname{tr}(\Gamma\, W) \leq \bar{\gamma} \\ & (15), (16) \end{aligned} \tag{18}$$

along Z*,* X*,* K*,* Q*,* P*,* Γ *and* Υ *and we define* $L = Z^{-1} X$*.*

Remark 10. *Although we assume that the system* (1) *is not affected by non-zero mean disturbances, it is possible to extend the results presented in this work to a system in the form of*

$$\begin{aligned} x_{k+1} &= A\, x_k + B\, u_k + E\, f_k + S\, w_k + S_2\, d_k, \\ y_k &= C\, x_k + D\, u_k + F\, f_k + T\, w_k + T_2\, d_k, \end{aligned}$$

where $d \in \mathbb{R}^{n_d}$ is a bounded vector and S_2 and T_2 are known constant matrices of appropriate dimensions. For such cases, we propose to obtain the matrix inequalities which bound the $\mathcal{H}_\infty$ norm of the dynamics between d and $\tilde{f}$ and add them in the design strategies of the observer. See [9] for details on obtaining this norm using standard matrix inequalities formulation. If unknown input decoupling were necessary, one could guarantee it by constraining the value of this $\mathcal{H}_\infty$ norm to zero or by using the algebraic constraints explained in [33,41]. To build this Unknown Input Observer (UIO), the rank inequalities in Assumptions 4 and 5 should be extended as indicated in [33].

5 Analysis of the Tracking Behavior of PMIR Observers

In this section, we analyze the tracking behavior of PMIR observers when the system is affected by different types of faults. For this analysis, we omit the effect of the noise w on the fault estimates.

5.1 Steady-state Analysis

From a steady-state perspective, we have shown that an observer in the form of (8) designed through the strategies presented in Section 4 experiences a finite cumulative squared error when any fault in the form of (2) affects the system. Thus, in such cases, the steady-state estimation error is zero. However, seldom is the dynamics of the real faults completely known and it is possible that the real dynamics of a fault affecting the system does not match the assumed model. In the following, we analyze the behavior of the estimator when the system is affected by any polynomial fault and by a sinusoidal fault of any frequency.

5.1.1 Polynomial Faults

Let us characterize the steady-state behavior of the PMIR observer (8) when the system (1) is affected by a polynomial fault of any degree N. To do so, we first introduce a corollary to Theorem 2 which gives a bound of the RMS-norm of the fault estimation error as a function of the difference between the degree of the fault (N) and the number of integral terms considered by the PMIR observer (n_I). Then, we obtain a bound of the final value of the estimation error.

Corollary 2. *Consider the fault estimator* (8) *applied to the system* (6). *If a fault $f[l]$ in the form of $f_k[l] = c_{N,l}\, k^{N-1}$ affects the system, the RMS norm of the l-th fault estimation error is bounded as*

$$\left\|\tilde{f}[l]\right\|_{RMS} \leq \begin{cases} 0 & \text{if } N \leq n_I \\ \chi_l\, c_{N,l} & \text{if } N = n_I + 1 \\ \infty & \text{if } N > n_I + 1 \end{cases}, \tag{19}$$

with $\chi_l = \left\|G_{\tilde{f}[l],\zeta[l]}(z)\right\|_\infty$ being the $\mathcal{H}_\infty$ norm of the transfer function between $\tilde{f}[l](z)$ and $\zeta[l](z)$ (i.e., the generating signal for the polynomial term of highest order $c_{n_I,l}\, k^{n_I-1}$).

Proof. Provided (5) and Remark 4, we have that $f_k[l] = c_{N,l}\, k^{N-1}$ (whose $\mathcal{Z}$ transform is $f[l](z) = \frac{c_{N,l}}{(1-z^{-1})^N}$) can be generated as

$$f[l](z) = G_{f[l],\zeta[\bar{m}]}(z)\, \zeta[\bar{m}](z)$$

with

$$\zeta[\bar{m}](z) = \frac{c_{N,l}}{(1-z^{-1})^{N-i}}$$

for any $i = 1, \dots n_I$ (index $\bar{m}$ being equivalent to $\bar{m}(i,l) \triangleq (n_I - i)\, n_f + l$). From Theorem 2 we have that $\left\|G_{\tilde{f},\zeta[m]}(z)\right\|_2^2 \leq \Upsilon[m,m]$ and, thus, $\left\|G_{\tilde{f}[l],\zeta[m]}(z)\right\|_\infty = \chi_m < \infty$. Then, the RMS norm of $\tilde{f}[l]$ is bounded as

$$\left\|\tilde{f}[l]\right\|_{RMS} \leq \chi_{\bar{m}} \left\|\mathcal{Z}^{-1}\left\{\frac{c_{N,l}}{(1-z^{-1})^{N-i}}\right\}\right\|_{RMS}$$

for all $i = 1, \ldots, n_I$ and it, thus, verifies

$$\left\|\tilde{f}[l]\right\|_{RMS} \leq \min_{i=1,\ldots,n_I} \left\{ \chi_{\bar{m}} \left\| \mathcal{Z}^{-1} \left\{ \frac{c_{N,l}}{(1-z^{-1})^{N-i}} \right\} \right\|_{RMS} \right\}.$$

The RMS norm of the signal $\mathcal{Z}^{-1}\left\{\frac{c_{N,l}}{(1-z^{-1})^{N-i}}\right\}$ is zero if $N-i<1$, finite if $N-i=1$ (i.e., a step signal), and infinite if $N-i>1$. Thus, the previous minimum is archived for $i=n_I$ and we have

$$\left\|\tilde{f}[l]\right\|_{RMS} \leq \chi_l \left\| \mathcal{Z}^{-1} \left\{ \frac{c_{N,l}}{(1-z^{-1})^{N-n_I}} \right\} \right\|_{RMS}.$$

because $\bar{m}(n_I, l) = l$, leading to the statement in Corollary 2. □

The bound (19) in Corollary 2 implies that if a fault $f[l]$ in the form of $f_k[l] = c_{N,l}\, k^{N-1}$ affects the system, the steady-state fault estimation error of the l-th fault, i.e., $\lim_{k\to\infty} \tilde{f}_k[l]$, is bounded as

$$\lim_{k\to\infty} \tilde{f}_k[l] \leq \begin{cases} 0 & \text{if } N \leq n_I \\ K_l & \text{if } N = n_I + 1 \\ \infty & \text{if } N > n_I + 1 \end{cases}, \tag{20}$$

with K_l a constant which can be obtained through the following procedure.

From Theorem 2 we have that $\left\|G_{\tilde{f},\zeta[m]}(z)\right\|_2^2 \leq \Upsilon[m,m]$ and, thus, $\left\|G_{\tilde{f}[l],\zeta[m]}(z)\right\|_2 = \phi_m < \infty$. Provided that

$$G_{\tilde{f}[l],\zeta[m]}(z) = G_{\tilde{f}[l],f[l]}(z)\, G_{f[l],\zeta[m]}(z)$$

and using the definition of $G_{f[l],\zeta[m]}(z)$ in (5), we have that

$$\left\|G_{\tilde{f}[l],\zeta[\bar{m}]}(z)\right\|_2 = \left\| G_{\tilde{f}[l],f[l]}(z)\, \frac{1}{(1-z^{-1})^i} \right\|_2 = \phi_m < \infty$$

for all $i = 1, \ldots n_I$ (index $\bar{m}$ being equivalent to $\bar{m}(i,l) \triangleq (n_I - i)\, n_f + l$). Thus, we deduce that $\lim_{k\to\infty} \tilde{f}_k[l] = 0$ when $\zeta_k[\bar{m}] = c_{i,l}\delta_k$. Applying the final value theorem, this result implies that

$$\lim_{z\to 1} G_{\tilde{f}[l],f[l]}(z)\, \frac{c_{i,l}}{(1-z^{-1})^{i-1}} = 0, \tag{21}$$

for all $i = 1, \ldots, n_I$. Let us now decompose $G_{\tilde{f}[l],f[l]}(z)$ as

$$G_{\tilde{f}[l],f[l]}(z) = \mathcal{H}_{l,l}(z)\, (1-z^{-1})^p,$$

where $\mathcal{H}_{l,l}(z)$ is a transfer function verifying $\mathcal{H}_{l,l}(1) = \kappa_{l,l}$ ($\kappa_{l,l}$ being a constant) and p represents the number of zeros at $z=1$ in $G_{\tilde{f}[l],f[l]}(z)$. Provided that

$$\lim_{z\to 1} \frac{\bar{K}\,(1-z^{-1})^p}{(1-z^{-1})^q} = \begin{cases} 0 & \text{if } q < p \\ \bar{K} & \text{if } q = p \\ \infty & \text{if } q > p \end{cases},$$

we deduce from (21) that

$$p \geq n_I \tag{22}$$

because $p \geq i$ for all $i = 1, \ldots, n_I$. Applying the final value theorem when a fault $f[l]$ in the form of $f_k[l] = c_{N,l}\, k^{N-1}$ affects the system, we get

$$\begin{aligned} &\lim_{z\to 1} G_{\tilde{f}[l],f[l]}(z)\, \frac{c_{N,l}}{(1-z^{-1})^{N-1}} = \\ &\lim_{z\to 1} \mathcal{H}_{l,l}(z) \frac{c_{N,l}(1-z^{-1})^p}{(1-z^{-1})^{N-1}} \leq \begin{cases} 0 & \text{if } N \leq n_I \\ \kappa_{l,l}\, c_{N,l} & \text{if } N = n_I + 1 \\ \infty & \text{if } N > n_I + 1 \end{cases} \end{aligned} \tag{23}$$

and we deduce that K_l in (20) satisfies $K_l = \kappa_{l,l}\, c_{N,l}$.

Remark 11. *In essence, the purpose of a fault estimator is to invert the transfer functions from the faults to the measurements [41]. If these transfer functions contain poles which are close to $z = 1$ (i.e., integrators), it may occur that the transfer function from a fault to the corresponding fault estimation error contains p_0 zeros at $z = 1$ (i.e., derivative terms) regardless of the dynamics of the faults included in the estimator. Thus, we rewrite* (22) *as $p = n_I + p_0$ with $p_0 \geq 0$ and we have that*

$$\lim_{z\to 1} G_{\tilde{f}[l],f[l]}(z)\,\frac{c_{N,l}}{(1-z^{-1})^{N-1}} =$$

$$\lim_{z\to 1} \mathcal{H}_{l,l}(z)\frac{c_{N,l}(1-z^{-1})^{n_I+p_0}}{(1-z^{-1})^{N-1}} = \begin{cases} 0 & \text{if } N \leq n_I+p_0 \\ K_l & \text{if } N = n_I+p_0+1 \\ \infty & \text{if } N > n_I+p_0+1 \end{cases}$$

with $K_l = \kappa_{l,l}\, c_{N,l}$. Since no a priori knowledge of $p_0 \geq 0$ is available, this equality leads to the bound (23).

5.1.2 Sinusoidal Faults

Let us now characterize the steady-state behavior of the PMIR observer (8) when the system (1) is affected by a sinusoidal fault of any frequency ω_N. To do so, we introduce a corollary to Theorem 2 which gives a bound of the RMS-norm of the fault estimation error through the difference between the frequency of the fault (ω_N) and the frequencies considered by the PMIR observer ($\omega_r,\ r = 1, \ldots, n_R$). From this bound, we deduce a bound of the steady-state fault estimation error.

Corollary 3. *Consider the fault estimator* (8) *applied to the system* (6). *If a fault $f[l]$ in the form of $f_k[l] = d_{N,l}\sin(\omega_N\, k)$ affects the system, the RMS norm of the l-th fault estimation error is bounded as*

$$\left\|\tilde{f}[l]\right\|_{RMS} \leq \begin{cases} 0 & \text{if } \omega_N \in \mho \\ \min\limits_{r=1,\ldots,n_R} \left\{\chi_{\breve{m}}\, \frac{d_{N,l}\,|\omega_r^2-\omega_N^2|}{\sqrt{2}\,\omega_N}\right\} & \text{if } \omega_N \notin \mho \end{cases} \tag{24}$$

with $\mho = \{\omega_1, \ldots, \omega_{n_R}\}$, $\chi_m = \left\|G_{\tilde{f}[l],\zeta[m]}(z)\right\|_\infty$ being the $\mathcal{H}_\infty$ norm of the transfer function between $\tilde{f}[l](z)$ and $\zeta[m](z)$ and index $\breve{m}$ being equivalent to $\breve{m}(r,l) \triangleq (n_I + n_R - r)\, n_f + l$.

Proof. According to the proof of Corollary 2, $f_k[l] = d_{N,l}\sin(\omega_N\, k)$ (whose $\mathcal{Z}$ transform is $f[l](z) = \frac{d_{N,l}\sin(\omega_N)\, z^{-1}}{1-2\,\cos(\omega_N)\, z^{-1}+z^{-2}}$) can be generated through $G_{f[l],\zeta[\breve{m}]}(z)$ by

$$\zeta[\breve{m}](z) = \frac{1-2\,\cos(\omega_r)\, z^{-1}+z^{-2}}{\sin(\omega_r)\, z^{-1}}\,\frac{d_{N,l}\sin(\omega_N)\, z^{-1}}{1-2\,\cos(\omega_N)\, z^{-1}+z^{-2}}.$$

for any $r = 1, \ldots n_R$ (index $\breve{m}$ being equivalent to $\breve{m}(r,l) \triangleq (n_I + n_R - r)\, n_f + l$). The RMS norm of $\tilde{f}[l]$ is thus bounded as

$$\left\|\tilde{f}[l]\right\|_{RMS} \leq \min_{r=1,\ldots,n_R} \left\{\chi_{\breve{m}}\, \left\|\mathcal{Z}^{-1}\left\{\zeta[\breve{m}](z)\right\}\right\|_{RMS}\right\}$$

which is equivalent to

$$\left\|\tilde{f}[l]\right\|_{RMS} \leq \min_{r=1,\ldots,n_R} \left\{\chi_{\breve{m}}\, \frac{d_{N,l}\,|\omega_r^2-\omega_N^2|}{\sqrt{2}\,\omega_N}\right\}$$

leading to the statement in Corollary 3. □

It is straightforward to deduce that the bound (24) in Corollary 3 implies that if a fault $f[l]$ in the form of $f_k[l] = d_{N,l}\sin(\omega_N\, k)$ affects the system, the peak value of the steady-state estimation error of the l-th fault, i.e., $\tilde{f}_k[l]$ with k sufficiently large to achieve the sinusoidal steady state, is bounded as ($\mho = \{\omega_1, \ldots, \omega_{n_R}\}$):

$$\max_k |\tilde{f}_k[l]| \leq \begin{cases} 0 & \text{if } \omega_N \in \mho \\ \min\limits_{r=1,\ldots,n_R} \left\{\chi_{\bar{\breve{m}}(r,l)}\, \frac{d_{N,l}\,|\omega_r^2-\omega_N^2|}{\omega_N}\right\} & \text{if } \omega_N \notin \mho \end{cases}$$

5.2 Transient Analysis

From the analysis in Section 5.1.1, we deduce that, from a steady-state perspective, better results are achieved when the degree n_I of the faults considered by the estimator is increased. However, increasing this degree has its counterpart in the transient behavior of the estimator. First, from (21) we have that

$$\lim_{z\to 1} \frac{1}{(1-z^{-1})^q}\, \mathcal{G}_{\tilde{f}[l],f[l]}(z)\, \frac{1}{(1-z^{-1})^{N-1}} = 0, \;\; \forall q \leq n_I - N$$

This equality implies that the cumulative error related to the l-th fault is zero whenever $N < n_I$ and that the fault estimate $\hat{f}[l]$ has, thus, an oscillatory behavior. It is worth nothing mentioning that this behavior is undesirable in fault estimation; especially, when the resulting fault estimates are used in fault tolerant control schemes.

Remark 12. *Likewise to the analysis performed in Remark 11, if we denote the number zeros at $z = 1$ which appear in the estimator regardless of the dynamics of the modeled faults as p_0, the equality in 5.2 holds for all $q \leq n_I + p_0 - N$.*

Second and considering $n_R = 0$, the design freedom of an observer in the form of (8) is provided by the observer gains $K \in \mathbb{R}^{n_f \times n_y}$ and $L = \begin{bmatrix} L_x \\ L_I \end{bmatrix}$ with $L_x \in \mathbb{R}^{n_x \times n_y}$ and $L_I \in \mathbb{R}^{(n_I \cdot n_f)\times n_y}$. In general and omitting the design effort which is devoted to the satisfaction of noise attenuation constraints, all the design flexibility provided by L_x, L_I and K can be used to ameliorate the ability to track the n_I polynomial terms of the faults. Now, if we design an augmented observer including polynomial faults up to degree $n_I + N$ in its model, the observer gains become K and $L' = \begin{bmatrix} L_x \\ L_N \\ L_I \end{bmatrix}$ with $L_N \in \mathbb{R}^{(N \cdot n_f)\times n_y}$. In such a case and given the structure of the matrices A_F, B_F and C_F in (4), the design freedom provided by L_I, L_x and K can be used to ameliorate the ability to track both the first n_I and the last N polynomial terms of the faults. For its part, the design flexibility provided by L_N has no effect on the ability to track the n_I polynomial terms of lower order and and it can only be used to improve the ability to track the N polynomial terms of higher order. In all, we intuitively deduce that the ability to track certain term of a polynomial fault cannot be improved by increasing the order of the augmented observer and that this tracking ability deteriorates as the sensitivity to polynomial terms of higher order is increased. Similar deductions apply to the number of resonators included in a PMIR observer.

5.3 Relevance of the Proposed Design

In this section, we have proved the exiting trade-off between the steady-state accuracy of an augmented observer w.r.t. complex faults and its transient behaviour w.r.t. simpler faults. For PMI observers, we have proved that if we choose a large observer order as proposed in the literature [16, 17], the steady-state error is effectively zero for polynomial faults below or equal to this order. It is constant for polynomial faults of one extra order and increasing for polynomial faults of higher-orders (Section 5.1.1). However, we have shown that this election imposes some compromises because it deteriorates the performance of the observer w.r.t. lower-order faults causing a slower and oscillatory response (Section 5.2).

This conclusion motivates the design proposed in Section 4 which, in contrast to the existing designs in the literature of augmented observers (e.g., [16, 40]), weights the effect of each polynomial degree of the fault. The weighting allows attenuating the negative effect on the transient behaviour of the observer w.r.t. low-order faults when extending the observer for taking into account more complex but less probable fault dynamics.

Moreover, the resonant terms that we propose to include in the PMI observer (leading to a PMIR observer) allow considering high-frequency faults without intensively augmenting the negative effect of the noises on the fault estimates. The PMIR architecture maximizes the observer fault sensitivity around the high-frequencies in which the sinusoidal fault terms are subject to occur. It should also be noted that the existence conditions for PMR observers differ from those of PMI observers (see Theorem 1). Thus, it would be possible to design a PMR observer for some systems which do not verify PMI observer existence conditions.

Table 1: Estimation errors of the PMI observers ($\bar{\gamma} = 0.010$).

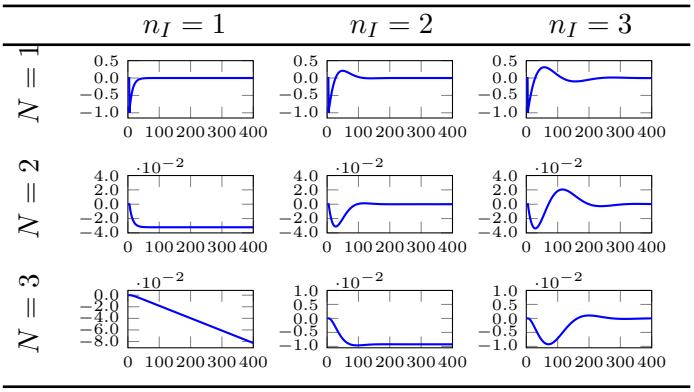

In all, compared with the existing literature of augmented observers, the proposed observer and its design are based on taking these performance trade-offs into account. They allow weighting the effect of the different fault terms according to their the probability of appearance or hazard and they make possible the estimation of resonant fault terms with higher noise attenuation levels.

Example 1. *To illustrate the goodness of the approach, consider the example case in which a system is prone to three kinds of faults: a step, a ramp and a sinus of certain high-frequency. We assume that the step and the sinusoidal fault have a high hazard potential due to their abrupt nature whilst the ramp fault is less damaging. A common PMI observer needs to consider two integrators of equal importance in its architecture and to accept low noise attenuation so as to capture the sinusoidal fault. The proposed PMIR observer is able to achieve higher noises attenuations because the resonant term enhances the sinusoidal fault sensitivity. Moreover, for an equal noise attenuation level, faster step fault tracking can be achieved at the cost of a slower response to the less dangerous ramp fault.*

Let us finally remark that the proposed observer does not introduce any complexity in terms of implementation because its architecture is analogous to that of PI and PMI observers. Note that augmented observers are not highly computationally demanding because they avoid complex schemes and computations (e.g., the adaptive laws in [4] involving nonlinear computations or the intermediate computation steps of the iterative observer in [6]). In terms of design, the procedure is based on standard convex optimization problems with LMIS. Moreover, the tuning of the constraining terms in the design is facilitated by the use of intuitive parameters (variances and CSEs).

6 Numerical Illustrative Example

In this section, we numerically show the effects caused by large-order augmented observers and the advantages of weighting the effect of the different fault dynamics included in the observer. Moreover, we study the convenience of including resonant terms in the augmented observer when the system is prone to high-frequency faults. For this purpose, consider a system in the form of (1) with

$$A = \begin{bmatrix} 0.700 & 0.300 & 0.200 & -0.003 \\ 0.050 & 0.600 & -0.002 & -0.040 \\ 0.010 & 0.003 & 0.630 & 1 \\ 0 & 0 & 0.010 & 0.600 \end{bmatrix}, \quad B = \begin{bmatrix} 0.0044 & 0.0018 \\ 0.0353 & -0.0755 \\ -0.0559 & 0.0454 \\ -0.0003 & 0.0002 \end{bmatrix}, \quad C = \begin{bmatrix} 1 & 0 & 0 & 0 \\ 0 & -1 & 0 & 0 \end{bmatrix},$$

$$D = 0_{2\times 2}, \quad S = \begin{bmatrix} I_4 & 0_{4\times 2} \end{bmatrix}, \quad T = \begin{bmatrix} 0_{2\times 4} & I_2 \end{bmatrix}.$$

The covariance matrix of the noises is $W = 0.004\, I_6$. In the following, we study the case in which this system is only affected by actuator faults and the case in which it is prone to both actuator and sensor faults. For sake

Table 2: Characterization of the PMI observers ($m = n_I - i + 1$).

PMI					
$\bar{\gamma} = 0.010$					
CODE	I1	I2	I2-L	I2-M	I2-H
n_I	1	2	2	2	2
$\bar{\upsilon}_m(i=1)$	-	-	6.20	5.30	4.87
$\upsilon_m\ (i=1)$	4.87	7.28	6.12	5.28	4.87
$\upsilon_m\ (i=2)$	-	3001	3445	6740	566645
$\bar{\gamma} = 0.005$					
CODE	I1	I2	I2-L	I2-M	I2-H
n_I	1	2	2	2	2
$\bar{\upsilon}_m\ (i=1)$	-	-	12.50	10.80	9.70
$\upsilon_m\ (i=1)$	9.67	14.51	12.47	10.78	9.70
$\upsilon_m\ (i=2)$	-	24174	26790	43623	1167520

of clarity, unless explicitly stated otherwise, we show the simulation results with $w_k = 0$. The latter does not mean that $w_k = 0$; it only means that we remove the effect of the noises in the figures. For sake of brevity, we do not include the obtained observer gain matrices. All the observer designs are set up in YALMIP [42] and solved using the solver MOSEK [43].

6.1 Actuator Fault

Suppose that the system has the following fault distribution matrices

$$E = \begin{bmatrix} -0.0088 & -0.0706 & 0.1118 & 0.0006 \end{bmatrix}^T, \ \ F = \begin{bmatrix} 0 & 0 \end{bmatrix}^T,$$

and define the following polynomial fault signals (all of them appearing at $k = 5$ and reaching $f_k = 1$ at $k = 305$):

$$f_{k(N=1)} = \begin{cases} 1 & \text{if } \ k \geq 5 \\ 0 & \text{otherwise} \end{cases}, \tag{25a}$$

$$f_{k(N=2)} = \begin{cases} \frac{1}{300}\,(k-5) & \text{if } \ k \geq 5 \\ 0 & \text{otherwise} \end{cases}, \tag{25b}$$

$$f_{k(N=3)} = \begin{cases} \frac{1}{300^2}\,(k-5)^2 & \text{if } \ k \geq 5 \\ 0 & \text{otherwise} \end{cases}. \tag{25c}$$

Define also the following sinusoidal faults (appearing at $k = 5$):

$$f_{k(\omega_N=\omega_1)} = \begin{cases} \sin[\omega_1\,(k-5)] & \text{if } \ k \geq 5 \\ 0 & \text{otherwise} \end{cases}, \tag{26a}$$

$$f_{k(\omega_N=\omega_2)} = \begin{cases} \sin[\omega_2\,(k-5)] & \text{if } \ k \geq 5 \\ 0 & \text{otherwise} \end{cases}. \tag{26b}$$

with $\omega_1 = 0.24$ rad/sample and $\omega_2 = 2\,\omega_1 = 0.48$ rad/sample.

6.1.1 PMI Observers

Let us design PMI observers (i.e., PMIR observers with $n_R = 0$) for different values of n_I ($n_I = 1, 2, 3$). We follow the Strategy 2 presented in Section 4.3 with a variance noise constraint equal to $\bar{\gamma} = 0.010$. First, we minimize the expected CSE of all the unitary impulse inputs $\zeta[m]$ considering that they have an equal probability of appearance (i.e., $\Omega = [1, n_\zeta]$ and $\alpha_m = 1$ for all m). Table 1 includes the fault estimation error $\tilde{f}$ experienced

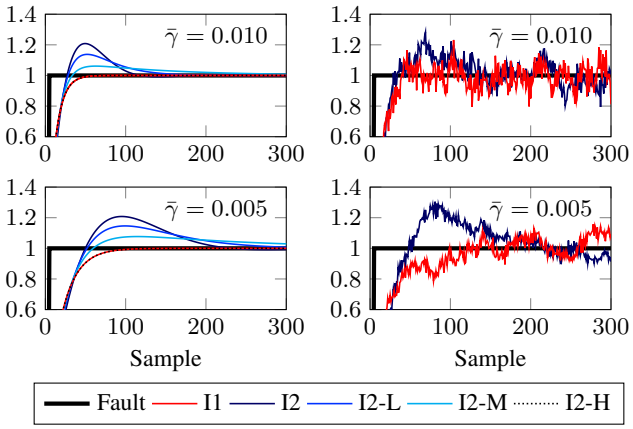

Figure 1: Step fault estimation via different PMI observers (Table 2) with different noise attenuation constraints. Left: $w_k = 0$. Rigth: ($w_k \neq 0$)

Table 3: Characterization of the PMR observers ($m = n_I + n_r - r + 1$).

PMR					
$\bar{\gamma} = 0.010$					
CODE	R1	R2	R2-L	R2-M	R2-H
n_R	1	2	2	2	2
$\bar{\upsilon}_m(r=1)$	-	-	7.00	5.70	4.38
$\upsilon_m(r=1)$	4.37	8.31	7.00	5.70	4.38
$\upsilon_m\ (r=2)$	-	8.10	10.04	15.55	1727
$\bar{\gamma} = 0.005$					
CODE	R1	R2	R2-L	R2-M	R2-H
n_R	1	2	2	2	2
$\bar{\upsilon}_m(r=1)$	-	-	14.00	11.50	8.97
$\upsilon_m\ (r=1)$	8.95	16.65	14.00	11.50	8.97
$\upsilon_m\ (r=2)$	-	15.91	19.88	30.74	2804

by each observer when the system is subject to each of the polynomial faults (25) (i.e., $f_k = f_{k(N)}$ with $N = 1, 2, 3$). We prove that, as detailed in Section 5.1, the steady-state error is zero whenever $N \leq n_I$, it is constant if $N = n_I + 1$ and it is unbounded if $N > n_I + 1$. The counterpart of augmenting the order of the observer is also shown in the table: the transient behavior becomes more oscillatory as the difference between n_I and N increases (see Section 5.2).

Moreover, the results in Table 2 show that the CSE experienced under step faults (denoted as $\upsilon_m(i=1)$) is lower with $n_I = 1$ (observer I1) than with $n_I = 2$ (observer I2), being 4.78 vs. 7.28. Then, when step faults occur, I1 behaves better than I2 at the cost of non-zero steady-state estimation errors towards ramp faults.

As proposed in Section 5, intermediate solutions can be achieved by designing observers with $n_I = 2$ and adding a constraint on the CSE due to step faults. To do so, we follow the same design strategy (Strategy 2 with $\bar{\gamma} = 0.010$) and we constrain the CSE regarding the lower-order integrator. Note that this design is equivalent to the one minimizing the expected CSE of all fault terms with a higher probability of appearance in the lower-order fault terms. Table 2 includes the obtained results. Here, $\bar{\upsilon}_m$ stands for the value of the step CSE constraint (i.e., $\Upsilon[m, m] < \bar{\upsilon}_m$). As this constraint becomes more restrictive (from I2-L to I2-H), the performance of the observer w.r.t. step faults is closer to the performance of a PMI observer with one integrator (I1), but at the cost of worsening the performance w.r.t to ramps (see the values of the CSE experienced under ramp faults denoted as $\upsilon_m(i=2)$). Note that for the most restrictive feasible constraint (i.e, $\bar{\upsilon}_{n_I}$ for $n_I = 2$ equals the value of υ_{n_I} for $n_I = 1$), the performance of the resulting observer (I2-H) w.r.t. step faults equals the performance of I1.

For its part, when imposing more restrictive noise attenuation constraints in the design ($\bar{\gamma} = 0.005$), the CSEs

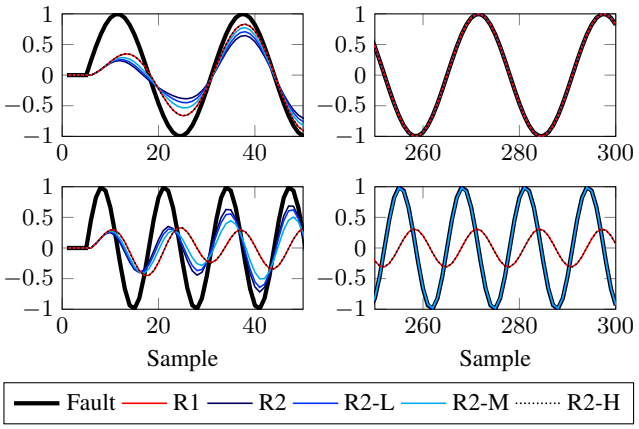

Figure 2: Transient and steady-state fault estimation via different PMR observers (Table 3 and $\bar{\gamma} = 0.010$) under two sinusoidal faults of frequencies ω_1 and ω_2.

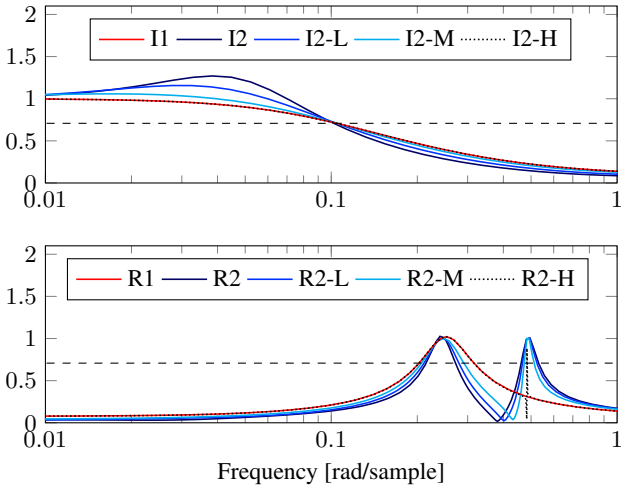

Figure 3: Magnitude of the closed-loop transfer function between f and $\hat{f}$ for different PMI and PMR observers (Tables 2 and 3, $\bar{\gamma} = 0.010$).

increase and the fault tracking ability of the observers deteriorates for improving the accuracy of the estimates w.r.t. the noises.

Fig.1 shows these trade-offs when simulating the step fault defined in (25a). We verify that the response of the observers with $n_I = 2$ approach the response of the observer with $n_I = 1$ as the CSE step fault constraint becomes more restrictive. We also verify that if the estimates becomes less noisy (with a more restrictive constraint $\bar{\gamma}$), the responses w.r.t. to faults become slower.

6.1.2 PMR Observers

Let us now design PMR observers (i.e., PMIR observers with $n_I = 0$) for $n_R = 1, 2$ (with $\omega_1 = 0.24$ rad/sample and $\omega_2 = 2\,\omega_1$) following the same strategy (i.e., Strategy 2 in Section 4.3). Similar deductions as the ones developed for PMI observers hold for PMR observers. The numerical results in Table 3 show that increasing the number of resonators in the observer reduces its ability to track the lower-frequency terms which are also included in the observer. Thus, the CSE experienced under a sinusoidal fault of frequency ω_1 (denoted as $\bar{v}_m(r = 1)$) is smaller for the observer just including ω_1 (observer R1) than for the observer including both frequencies ω_1 and ω_2 (observer R2). Again, compromise solutions (R2-L,R2-M and R2-H) can be achieved by designing an observer with both frequencies and imposing a restriction regarding the CSE due to the sinusoidal fault of frequency ω_1 (denoted as $\bar{v}_m(r = 1)$ in the table). The results in Table 3 also show that higher noise attenuations

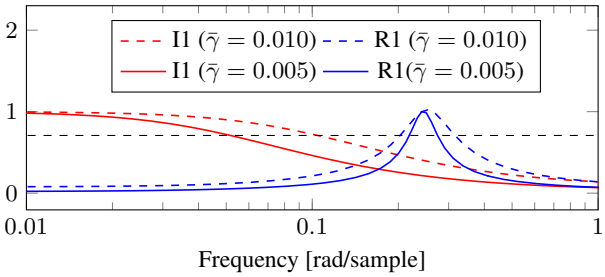

Figure 4: Magnitude of the closed-loop transfer function between f and $\hat{f}$ for different PMI and PMR observers (Tables 2 and 3) designed with different noise attenuation constraints.

(e.g., $\bar{\gamma} = 0.005$) impose larger CSEs.

Fig.2 includes the simulation results for these observers ($\bar{\gamma} = 0.010$) when the system is subject to the sinusoidal faults defined in (26). We verify the numerical results regarding the CSE in Table 3 and we prove that the steady-state error is only zero if the frequency ω_N defining the sinusoidal fault signal is within the frequencies ω_r included in the observer. Thus, if the fault is defined as (26a), the steady-state error is zero for both observers R1 (designed with $n_R = 1$) and R2 (designed with $n_R = 2$). Contrariwise, if the fault is defined as (26b), the steady-state error is only zero for R2.

6.1.3 Comparison of PMI and PMR Observers

Let us first obtain the frequency response of the closed-loop transfer function between f and $\hat{f}$ (denoted as $G_{\hat{f},f}$) for the observers in Table 2 and Table 3 with $\bar{\gamma} = 0.010$. Fig.3 depicts the magnitude of these frequency responses. We do not include the corresponding phase plots due to space constraints.

First, as deduced in Section 6.1.1, we verify that the behavior of the PMI observers with two integrators (I2, I2-L and I2-M) is oscillatory: the magnitude of the transfer function is larger than 1 for some low frequencies. We also corroborate that intermediate results between I1 and I2 can be achieved by constraining the CSE due to step faults as proposed in Section 4.3. Similar applies to PMR observers.

Fig.3 shows that the 3 dB bandwidth of PMI observers is much lower than ω_1 and ω_2 (0.1 vs. 0.24 and 0.48 rad/sample); thus, poor steady-state estimation results are obtained if we use PMI observers in order to track the pure high-frequency sinusoidal faults defined in (26). The unitary gain of $G_{\hat{f},f}$ for R1 at ω_1 ensures zero steady-state errors if the fault (26a) affects the system and the same applies to R2 w.r.t. the faults (26a) and (26b). Contrariwise, if a sinusoidal fault of low frequency (e.g., $0.2\omega_1 = 0.05$ rad/sample) occurs, PMI observers offer much better estimation results than PMR observers. Effectively, the gain of $G_{\hat{f},f}$ for R1 and R2 at low frequencies is barely zero. Fig.5 and Fig.6 illustrate these behaviours. The initial conditions in these simulation are fixed to $x_0 = \begin{bmatrix} 1 & 1 & 1 & 1 \end{bmatrix}$. As stated in Theorem 2, the simulation results show that the fault estimation error converges to zero in the absence of faults.

For its part, Fig.4 reveals the effect of the restrictiveness of the noise attenuation constraint included in the design. One verifies that higher noise attenuation constraints impose lower bandwidths. For I1 with $\bar{\gamma} = 0.010$, the 3 dB bandwidth is 0.09 rad/sample; and for I1 with $\bar{\gamma} = 0.005$, it is 0.05 rad/sample. Similarly, the 3 dB bandwidth for R1 reduces from 0.12 to 0.06 rad/sample if $\bar{\gamma}$ varies from 0.010 to 0.005. Hence, we deduce that PMI observers track faults of higher frequencies as the noise is less attenuated and we conclude that the use of the resonant terms proposed in this work allow to consider high-frequency faults without intensively augmenting the effect of the noise on the fault estimates.

From Fig.4 we also conclude that PMR observers are more robust against uncertainties in the real frequencies of the faults as the attenuation from the noise is reduced. Thus, if a sinusoidal fault of some frequency $(1+\delta)\,\omega_1$ affected the system, R1 with $\bar{\gamma} = 0.010$ would offer better fault tracking results than R1 with $\bar{\gamma} = 0.005$ at the cost of lower noise attenuation.

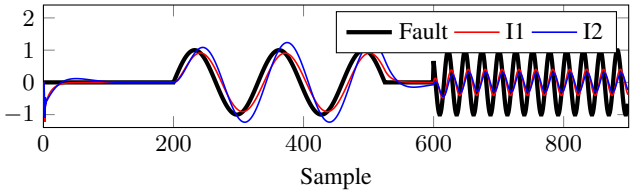

Figure 5: Estimation via different PMI observers (Table 2, $\bar{\gamma} = 0.010$) of two sinusoidal faults of frequencies $0.20\,\omega_1$ and ω_1.

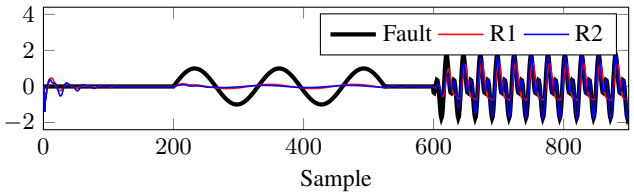

Figure 6: Estimation via different PMR observers (Table 3 and $\bar{\gamma} = 0.010$) of a sinusoidal fault of frequency $0.20\,\omega_1$ and another of frequencies ω_1 plus ω_2.

6.1.4 PMIR Observers

Let us now design PMIR observers through the Strategy 2 presented in Section 4.3 with different values of n_I and n_R ($\bar{\gamma} = 0.010$). Table 4 includes the CSE of these observers (υ_m) w.r.t. different fault terms. Again, we deduce that increasing the order of the observer deteriorates the transient performance of the estimator towards lower-order faults. Compromise solutions can be achieved by imposing a restriction regarding the lower-order CSE constraints. For instance, observer I1-R2 ($n_i = 1$ and $n_r = 2$) offers good results for the high-frequency sinus ($\upsilon_{\check{m}}$ $(r = 2)$ equals 11.98) and an intermediate performance for the low-frequency sinus ($\upsilon_{\check{m}}$ $(r = 1)$ equals 12.37) and for other low-frequency signals ($\upsilon_{\bar{m}}$ $(i = 1)$ equals 12.64). If better results regarding the low-frequency sinus were required, one could design an observer like I1-R2-R with a CSE constraint over the low-frequency sinus (with a value $\bar{\upsilon}_{\check{m}}(r = 1)$ equal to 9.25).

Fig.7 shows the fault estimation results provided by the observer I1-R1 (designed with $n_I = n_R = 1$) when the system is subject to either the step fault defined in (25a) or the sinusoidal fault defined in (26a). We prove that unlike the so-called PMI observer, this PMIR observer ensures zero steady-state estimation errors for both types of fault signals without increasing the noise effect. Effectively, the frequency response in the first part of Fig.8 shows that the observer I1-R1 ($n_I = n_R = 1$) offers a compromise performance between the performance of I1 ($n_I = 1$) and R1 ($n_R = 1$). The CSE w.r.t. the step fault is 8.93 (vs. 4.87 obtained for I1) and 8.53 w.r.t. the sinusoidal fault (vs. 4.37 obtained for R1).

6.2 Actuator and Sensor Fault

Consider the situation in which the system suffers from simultaneous actuator (f^a) and sensor (f^s) faults and let $f = \begin{bmatrix} f^a & f^s \end{bmatrix}^T$. Then, one gets accordingly the following distribution matrices ($n_f = 2$):

$$E = \begin{bmatrix} -0.0088 & -0.0706 & 0.1118 & 0.0006 \\ 0 & 0 & 0 & 0 \end{bmatrix}^T, \quad F = \begin{bmatrix} 0 & 0 \\ 1 & 0 \end{bmatrix}^T.$$

Table 4: CSE of the PMIR observers ($\bar{m}=n_I-i+1$, $\check{m}=n_I+n_r-r+1$).

PMIR					
$\bar{\gamma}=0.010$					
CODE	I1-R1	I1-R2	I1-R2-R	I2-R1	I2-R2
n_I	1	1	1	2	2
$\bar{v}_{\bar{m}}(i=1)$	-	-	-	-	-
$\bar{v}_{\bar{m}}(i=2)$	-	-	-	-	-
$v_{\bar{m}}(i=1)$	8.93	12.64	15.26	7.44	7.42
$v_{\bar{m}}\ (i=2)$	-	-	-	3164	3279
n_R	1	2	2	1	2
$\bar{v}_{\check{m}}(r=1)$	-	-	9.25	-	-
$\bar{v}_{\check{m}}(r=2)$	-	-	-	-	-
$v_{\check{m}}\ (r=1)$	8.53	12.37	9.23	186.79	200.20
$v_{\check{m}}\ (r=2)$	-	11.98	14.48	-	146.67

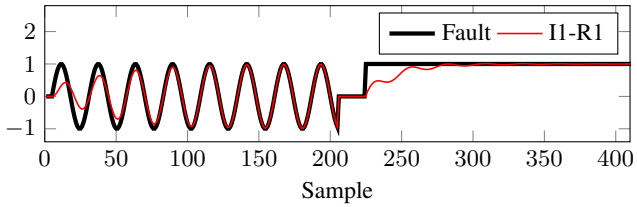

Figure 7: Estimation of a step and a sinusoidal fault (frequency ω_1) via a PMIR observer (Table 4).

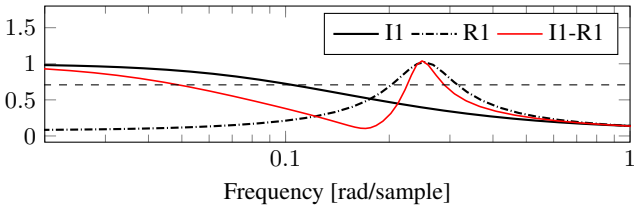

Figure 8: Frequency response of the closed-loop transfer function between f and $\hat{f}$ for different PMIR observers (Table 4 and $\bar{\gamma}=0.010$).

Define

$$f^a_{k(N=1)} = \begin{cases} 1 & \text{if } \ k \in [5, 500] \\ 0 & \text{otherwise} \end{cases}, \tag{27a}$$

$$f^s_{k(N=1)} = \begin{cases} 1 & \text{if } \ k \in [1005, 1500] \\ 0 & \text{otherwise} \end{cases}, \tag{27b}$$

$$f^s_{k(\omega_N=\omega_1)} = \begin{cases} \sin[\omega_1 (k-5)] & \text{if } \ k \in [5, 500] \\ 0 & \text{otherwise} \end{cases}. \tag{27c}$$

Let us design PMIR observers using the Strategy 2 with $\Omega=[1, n_\zeta]$ and $\alpha_m=1$ for all m. For $\bar{\gamma}=0.010$ and for $\bar{\gamma}=0.005$, we design the observers I1 (with $n_I=1$, $n_R=0$), I2 (with $n_I=2$, $n_R=0$), R1 (with $n_I=0$, $n_R=1$), R2 (with $n_I=0$, $n_R=2$) and I1-R1 (with $n_I=1$, $n_R=1$).

Fig.9 shows the results for $f_k=\begin{bmatrix} f^a_{k(N=1)} & f^s_{k(N=1)} \end{bmatrix}^T$. Note that deficits in the fault tracking behavior affect the fault isolation capability. As explained in Section 6.1, if the observer I2 is used, the actuator fault estimate experiences an oscillatory behavior when the step actuator fault occurs. Now, the sensor fault estimate does also experience a transient oscillatory deviation. If I1 ($n_i=1$ and $n_r=0$) is used instead, the transient deviation is

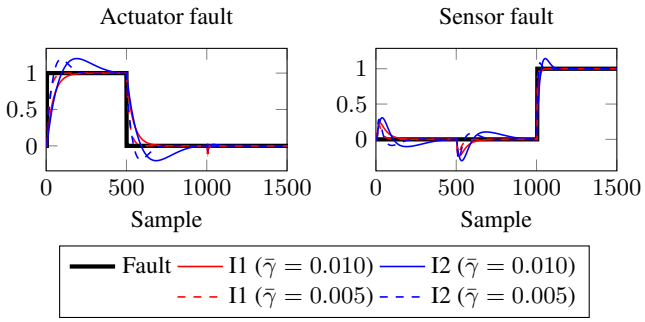

Figure 9: Estimation of step actuator and sensor faults via different PMI observers designed with different noise attenuation constraints.

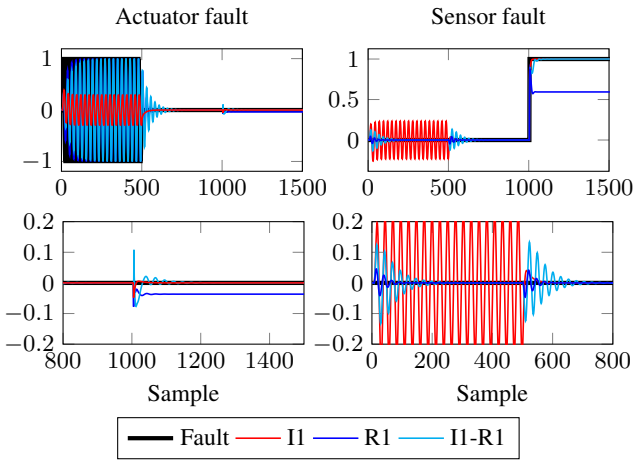

Figure 10: Fault estimation via different PMIR observers ($\bar{\gamma} = 0.010$) under a sinusoidal actuator fault (ω_1) and a step sensor fault.

not oscillatory and, thus, the isolation capability is improved during transients.

In order to analyze this effect from a steady-state perspective, assume now that $f_k = \left[f^a_{k(N=1)} \quad f^s_{k(\omega_N=\omega_1)}\right]^T$. The simulation results are shown in Fig.10. When the step actuator fault occurs, the observer I1 ($n_i = 1$ and $n_r = 0$) ensures zero steady-state estimation errors that enhance perfect fault isolation in steady state. However, when the sinusoidal sensor fault occurs, the steady-state estimation errors are non-zero and, thus, the fault isolation capability of the estimator is deteriorated. The opposite occurs if the observer R1 ($n_i = 0$ and $n_r = 1$) is used: perfect steady-state fault isolation is guaranteed when sinusoidal faults occur and the problems appear when step faults affect the system. Finally, the observer I1-R1 ($n_i = 1$ and $n_r = 1$) guarantees perfect steady-state fault isolation for both step and sinusoidal faults (see the details in the second part of Fig.10). Thus, we deduce that PMIR observers are useful if different types of faults appear all around the system. For instance, sensor faults may always represent biases (i.e., step faults). However, if sinusoidal actuator faults affect the system, the use of resonators for the sensor fault estimation guarantees perfect steady-state fault isolation and avoids the appearance of steady-state fault interactions.

7 Conclusion

In this work, we have generalized the standard formulation of a PMI observer to enhance the estimation of high-frequency fault signals. We have given the existence conditions of the novel observer and we have presented a multiobjective design strategy to fix an optimal trade-off between the variance of the estimations in fault-free scenarios and their cumulative squared tracking error in the presence of different faults. We have also studied the

influence of the complexity of the estimator (i.e., the order of the augmented observer) on the existing trade-off between the steady-state and transient tracking performance of the estimator when the system is subject to faults of different complexity. The design and the main conclusions of this study are validated when the proposed FE strategy is applied to a numerical illustrative example. The use of these fault estimates in active FTC strategies highlights as immediate future work. Future work will also apply the approach to practical engineering examples.

8 Acknowledgments

This work has been supported by the Spanish Ministry of Education, Culture and Sports (Grant no. FPU14/01592), the Spanish Ministry of Economy, Industry and Competitiveness (Project no. EC2015-69155-R) and the Universitat Jaume I (Project no. P11B2015-42).

References

[1] J. Chen and R. J. Patton, *Robust model-based fault diagnosis for dynamic systems*, vol. 3. Springer, 2012.

[2] Y. Zhang and J. Jiang, "Bibliographical review on reconfigurable fault-tolerant control systems," *Annual Reviews in Control*, vol. 32, no. 2, pp. 229–252, 2008.

[3] C. Edwards, S. K. Spurgeon, and R. J. Patton, "Sliding mode observers for fault detection and isolation," *Automatica*, vol. 36, no. 4, pp. 541–553, 2000.

[4] S. Fu, J. Qiu, L. Chen, and S. Mou, "Adaptive fuzzy observer design for a class of switched nonlinear systems with actuator and sensor faults," *IEEE Transactions on Fuzzy Systems*, 2018.

[5] D. Ye, M.-M. Chen, and H.-J. Yang, "Distributed adaptive event-triggered fault-tolerant consensus of multiagent systems with general linear dynamics," *IEEE Transactions on Cybernetics*, 2018.

[6] S.-J. Huang, D.-Q. Zhang, L.-D. Guo, and L.-B. Wu, "Convergent fault estimation for linear systems with faults and disturbances," *IEEE Transactions on Automatic Control*, vol. 63, no. 3, pp. 888–893, 2018.

[7] W. Chen and M. Saif, "An iterative learning observer for fault detection and accommodation in nonlinear time-delay systems," *International Journal of Robust and Nonlinear Control*, vol. 16, no. 1, pp. 1–19, 2006.

[8] Z. Gao, C. Cecati, and S. X. Ding, "A survey of fault diagnosis and fault-tolerant techniques – Part I: Fault diagnosis with model-based and signal-based approaches," *IEEE Transactions on Industrial Electronics*, vol. 62, no. 6, pp. 3757–3767, 2015.

[9] K. Zhang, B. Jiang, P. Shi, and V. Cocquempot, *Observer-Based Fault Estimation Techniques*. Springer, 2018.

[10] D. Koenig and S. Mammar, "Design of proportional-integral observer for unknown input descriptor systems," *IEEE Transactions on Automatic Control*, vol. 47, no. 12, pp. 2057–2062, 2002.

[11] A.-G. Wu and G.-R. Duan, "Generalized PI observer design for linear systems," *IMA Journal of Mathematical Control and Information*, vol. 25, no. 2, pp. 239–250, 2007.

[12] J.-W. Zhu and G.-H. Yang, "Fault-tolerant control for linear systems with multiple faults and disturbances based on augmented intermediate estimator," *IET Control Theory & Applications*, vol. 11, no. 2, pp. 164–172, 2016.

[13] K. Zhang, B. Jiang, and V. Cocquempot, "Robust fault estimation observer design with finite-time convergence specification," *IET Control Theory & Applications*, vol. 11, no. 1, pp. 1–9, 2016.

[14] Z. Gao and S. X. Ding, "Actuator fault robust estimation and fault-tolerant control for a class of nonlinear descriptor systems," *Automatica*, vol. 43, no. 5, pp. 912–920, 2007.

[15] A.-G. Wu, G.-R. Duan, and W. Liu, "Proportional multiple-integral observer design for continuous-time descriptor linear systems," *Asian Journal of Control*, vol. 14, no. 2, pp. 476–488, 2012.

[16] Z. Gao and S. X. Ding, "Fault estimation and fault-tolerant control for descriptor systems via proportional, multiple-integral and derivative observer design," *IET Control Theory & Applications*, vol. 1, no. 5, pp. 1208–1218, 2007.

[17] Z. Gao, S. X. Ding, and Y. Ma, "Robust fault estimation approach and its application in vehicle lateral dynamic systems," *Optimal Control Applications and Methods*, vol. 28, no. 3, pp. 143–156, 2007.

[18] C.-I. Chen and Y.-C. Chen, "Comparative study of harmonic and interharmonic estimation methods for stationary and time-varying signals," *IEEE Transactions on Industrial Electronics*, vol. 61, no. 1, pp. 397–404, 2014.

[19] B. Chen, G. Pin, W. N. Ng, S. Y. Hui, and T. Parisini, "An adaptive observer-based robust estimator of multi-sinusoidal signals," *IEEE Transactions on Automatic Control*, 2017.

[20] J. Na, J. Yang, X. Wu, and Y. Guo, "Robust adaptive parameter estimation of sinusoidal signals," *Automatica*, vol. 53, pp. 376–384, 2015.

[21] D. Robles, V. Puig, C. Ocampo-Martinez, and L. E. Garza-Castañón, "Reliable fault-tolerant model predictive control of drinking water transport networks," *Control Engineering Practice*, vol. 55, pp. 197–211, 2016.

[22] A. Kirakosyan, M. S. El Moursi, and V. Khadkikar, "Fault ride through and grid support topology for the VSC-HVDC connected offshore wind farms," *IEEE Transactions on Power Delivery*, vol. 32, no. 3, pp. 1592–1604, 2017.

[23] S. Aouaouda, M. Chadli, P. Shi, and H.-R. Karimi, "Discrete-time H_-/H_∞ sensor fault detection observer design for nonlinear systems with parameter uncertainty," *International Journal of Robust and Nonlinear Control*, vol. 25, no. 3, pp. 339–361, 2015.

[24] A. A. Stoorvogel, H. H. Niemann, A. Saberi, and P. Sannuti, "Optimal fault signal estimation," *International Journal of Robust and Nonlinear Control*, vol. 12, no. 8, pp. 697–727, 2002.

[25] M. Witczak, M. Buciakowski, V. Puig, D. Rotondo, and F. Nejjari, "An LMI approach to robust fault estimation for a class of nonlinear systems," *International Journal of Robust and Nonlinear Control*, vol. 26, no. 7, pp. 1530–1548, 2016.

[26] K. Zhang, B. Jiang, V. Cocquempot, and H. Zhang, "A framework of robust fault estimation observer design for continuous-time/discrete-time systems," *Optimal Control Applications and Methods*, vol. 34, no. 4, pp. 442–457, 2013.

[27] J.-L. Chang, "Applying discrete-time proportional integral observers for state and disturbance estimations," *IEEE Transactions on Automatic Control*, vol. 51, no. 5, pp. 814–818, 2006.

[28] Z. Gao, "Fault estimation and fault-tolerant control for discrete-time dynamic systems," *IEEE Transactions on Industrial Electronics*, vol. 62, no. 6, pp. 3874–3884, 2015.

[29] A.-G. Wu, G. Feng, and G.-R. Duan, "Proportional multiple-integral observer design for discrete-time descriptor linear systems," *International Journal of Systems Science*, vol. 43, no. 8, pp. 1492–1503, 2012.

[30] G. Shen, X. Zhu, J. Zhang, and D. Xu, "A new feedback method for PR current control of LCL-filter-based grid-connected inverter," *IEEE Transactions on Industrial Electronics*, vol. 57, no. 6, pp. 2033–2041, 2010.

[31] A. Timbus, M. Liserre, R. Teodorescu, P. Rodriguez, and F. Blaabjerg, "Evaluation of current controllers for distributed power generation systems," *IEEE Transactions on Power Electronics*, vol. 24, no. 3, pp. 654–664, 2009.

[32] R. J. Patton, "Fault-tolerant control," *Encyclopedia of Systems and Control*, pp. 422–428, 2015.

[33] Z. Gao, X. Liu, and M. Z. Chen, "Unknown input observer-based robust fault estimation for systems corrupted by partially decoupled disturbances," *IEEE Transactions on Industrial Electronics*, vol. 63, no. 4, pp. 2537–2547, 2016.

[34] T. Söderström, *Discrete-time stochastic systems: estimation and control*. Springer, 2012.

[35] T. M. Guerra, R. Márquez, A. Kruszewski, and M. Bernal, "h_∞ LMI-based observer design for nonlinear systems via takagi–sugeno models with unmeasured premise variables," *IEEE Transactions on Fuzzy Systems*, vol. 26, no. 3, pp. 1498–1509, 2018.

[36] K. Zhou, J. C. Doyle, and K. Glover, *Robust and optimal control*, vol. 40. Prentice hall New Jersey, 1996.

[37] C. Scherer, P. Gahinet, and M. Chilali, "Multiobjective output-feedback control via LMI optimization," *IEEE Transactions on Automatic Control*, vol. 42, no. 7, pp. 896–911, 1997.

[38] M. C. de Oliveira, J. Bernussou, and J. C. Geromel, "A new discrete-time robust stability condition," *Systems & Control Letters*, vol. 37, no. 4, pp. 261–265, 1999.

[39] L. E. Ghaoui, F. Oustry, and M. AitRami, "A cone complementarity linearization algorithm for static output-feedback and related problems," *IEEE Transactions on Automatic Control*, vol. 42, no. 8, pp. 1171–1176, 1997.

[40] P. Kühne, F. Pöschke, and H. Schulte, "Fault estimation and fault-tolerant control of the FAST NREL 5-MW reference wind turbine using a proportional multi-integral observer," *International Journal of Adaptive Control and Signal Processing*, 2017.

[41] S. X. Ding, *Model-based fault diagnosis techniques: design schemes, algorithms, and tools*. Springer, 2008.

[42] J. Lofberg, "YALMIP: A toolbox for modeling and optimization in MATLAB," in *IEEE International Symposium on Computer Aided Control Systems Design, 2004*, pp. 284–289, IEEE, 2004.

[43] A. Mosek, "The MOSEK optimization toolbox for MATLAB manual," 2015.